POLITECNICO DI TORINO
Repository ISTITUZIONALE

Low-Loss Reflective Intelligent Surface Based on Polarization-Rotation for 6G FR3 Band Applications

Original
Low-Loss Reflective Intelligent Surface Based on Polarization-Rotation for 6G FR3 Band Applications / Aktas, K., Tolin, E., Bahr, A., Vipiana, F.. - (2026), pp. 1-5. (2026 20th European Conference on Antennas and Propagation (EuCAP) Dublin (Ire) 19-24 April 2026) [10.23919/EuCAP68105.2026.11612425].

Availability:
This version is available at: 11583/3015788 since: 2026-09-22T10:18:11Z

Publisher:
IEEE

Published
DOI:10.23919/EuCAP68105.2026.11612425

Terms of use:

This article is made available under terms and conditions as specified in the corresponding bibliographic description in the repository

Publisher copyright
IEEE postprint/Author's Accepted Manuscript

©2026 IEEE. Personal use of this material is permitted. Permission from IEEE must be obtained for all other uses, in any current or future media, including reprinting/republishing this material for advertising or promotional purposes, creating new collecting works, for resale or lists, or reuse of any copyrighted component of this work in other works.

(Article begins on next page)

19 November 2026

Low-Loss Reflective Intelligent Surface Based on Polarization-Rotation for 6G FR3 Band Applications

Kaan Aktas*†, Enrico Tolin*, Achim Bahr*, Francesca Vipiana†
*Antenna and EM Modelling, IMST GmbH, 47475 Kamp-Lintfort, Germany, {kaan.aktas, enrico.tolin}@imst.de
†Dept. of Electronics and Telecommunications, Politecnico di Torino, 10129 Torino, Italy, francesca.vipiana@polito.it

***Abstract*—Addressing the need for efficient channel control in 6G networks, we introduce a novel 3-bit reflective intelligent surface (RIS) concept. It is compatible with low-cost FR4 printed circuit board technology and operates at the 7.125-8.4 GHz FR3 band. The core innovation proposed here is the use of internal reflections between a polarization rotator and a filter, which successfully enhances the phase shift up to 307°. The method allows an efficient unit cell design maintaining a high reflection coefficient above -0.9 dB. The final RIS panel demonstrates reliable beam steering up to 50°. It shows a minimal performance degradation, with a maximum amplitude difference below -1.1 dB relative to the theoretical scan loss.**

***Index Terms*—6G, beam scanning, FR3 band, metasurfaces, polarization rotation, RIS**

I. Introduction

The sixth generation (6G) of wireless technology aims to create intelligent, interconnected networks with ubiquitous connectivity [1]. This objective drives a future where data traffic is expected to exceed the capacity of current 5G systems [2]. To meet the demands for data rate (up to 1,000 Gbps), low latency and efficiency, RIS offer a groundbreaking solution. It fundamentally changes the wireless channel from a random, statistical medium into a controllable, deterministic one. By creating a direct, non-line-of-sight (NLOS) communication path that bypasses blockages, RIS ensures enhanced signal transmission and provides a highly compatible and scalable technology for existing infrastructure [1]. This technology is vital for utilizing the proposed FR3 band ($7-24$ GHz), which offers better throughput than sub-6 GHz and superior coverage compared to millimeter-wave bands [3].

The main purpose of an RIS is to deflect an incoming beam to a desired direction by adapting the correct phase profile on its surface calculated by generalized Snell's law [4]. A fixed beam RIS can be designed by using passive unit cells that rely on the geometry and dimensions of the copper-etched pattern to achieve a phase gradient surface [5], [6]. Although these passive cells can achieve high reflection coefficients with a phase range exceeding 340° [7], they also rely on resonance frequency. Consequently, the phase shift rapidly slopes downward or upward, making the phase response not fully linear across a large fractional bandwidth. A stable slope is crucial to achieve the desired beam deflection angle throughout the desired band. While unit cells based on meander lines offer a potential solution [8], they are sensitive to variations in both line length and spacing.

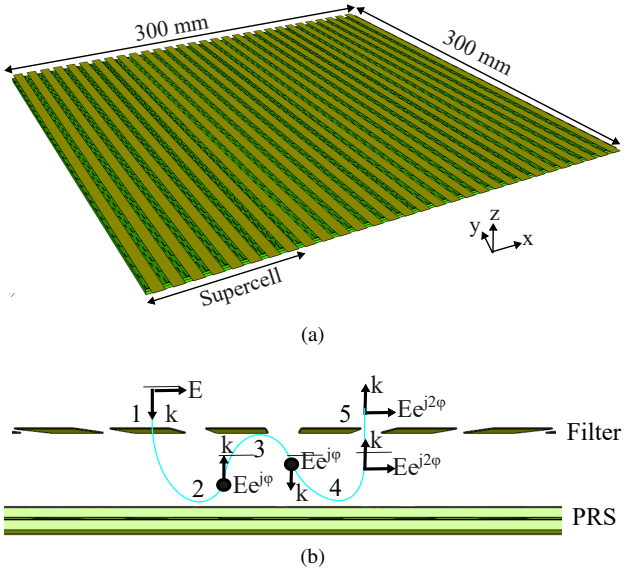


Fig. 1. (a) RIS panel configured for a 30° deflection. (b) Step-by-step visualization of the phase doubling concept using reflections. The flow (solid cyan line) shows the wave undergoing five steps, where additional phase φ is accumulated via reflections. PRS: Polarization rotating surface. k: wave vector. E: Electric field

Therefore, to achieve low loss design while providing also a linear phase range, here we propose a novel concept, illustrated in Fig. 1, which combines a polarization rotation unit cell and reflections from a polarization selective filter. In [9], [10] unit cells that combines filters and polarization rotations have been presented, but their application is limited to polarization control and does not extend to beam deflection through the phase adjustment. There are also researches on the usage of polarization-rotation unit cells in reflectarray antennas [11], [12]. However, these designs usually do not incorporate a filter concept. Instead, they manipulate the reflection phase by changing the orientation of the cells giving either 0° or 180° of phase. This provides a 1-bit solution which has lower resolution for the phase profile than using 3-bits.

The RIS, in this paper (Fig. 1), is designed to achieve 3-bit resolution and low loss performance using standard FR4 substrate. By utilizing FR4, we demonstrate a cost-effective and scalable design suitable for mass production. Instead of the conventional method of changing the orientation of the polarization rotation elements, we use a copper etching technique to achieve a continuous phase shift. Leveraging polarization

effects with an additional filter, allows the polarization rotator to operate with only half of the required phase range as depicted in Fig. 1. Benefiting from the reflections doubles the overall phase shift capacity aiming up to 315° in the low-FR3 band between 7.125 and 8.4 GHz [3]. Through this method, it is expected to achieve a more linear multi-bit phase response across a wide bandwidth while maintaining a high reflection amplitude. Therefore our novel concept provides an efficient RIS that is expected to be both cost-effective and high-performing despite lossy dielectric materials.

The paper is organized as follows. Section II introduces the concept and the proposed unit cell. It analysis in detail each component of the structure and their effects in the performance. Section III details the 3-bit RIS panel design, including its performance across the desired band and under various beam deflection angles. Finally, the paper concludes and discusses the future perspectives in Section IV.

II. RIS CONCEPT AND UNIT CELL DESIGN

A. Concept

RIS is composed of two main parts: a reflective polarization rotating surface (PRS) and a filter as depicted in Fig. 1(b). The core principle exploits the transmission of one polarization state and inter-reflections of the cross polarization state between PRS and the filter. This causes the wave to pass through the polarization rotation cells twice, thus doubles the reachable phase range. The phenomenon is illustrated in Fig. 1(b). A linearly polarized wave penetrates through the filter (step 1), then it interacts with a reflective polarization rotation surface (step 2). Each unit cell constructing the surface, changes the polarization to a cross polarized state and adds an additional phase value. Then, the wave front moving towards the filter bounces back (step 3) and re-interacts with unit cells (step 4). This converts it back to the initial polarization state and adds another phase value. Finally, the wave exits the filter with double the amount of phase value that a unit cell could provide (step 5). By leveraging this effect, polarization rotation unit cell only has to be designed to provide half of the total required phase range. This approach is expected to increase the linearity of the phase values and the overall efficiency of the unit cell, as the structure would rely less on deep resonances to achieve the full phase range.

B. Unit cell design

The performance of a split ring polarization rotator with a filter in [9] has already been demonstrated to achieve a high efficiency. In our work, we inspire from that idea and combine the phase shifting and polarization rotation on the same structure. The proposed unit cell design shown in Fig. 2 is composed of four layers: A metal strip on the top layer for filtering, underneath a 45° tilted split ring polarization rotator, beneath a ring resonator to improve the accuracy of phase and at the bottom layer a ground plane for reflection. The latter three layers constructing the main assembly, utilizes FR4 ($\epsilon_r = 4.3$, $\tan\delta = 0.01$) as the dielectric substrate. The filter layer though is separated by air. The period is $\lambda/3.85$ at

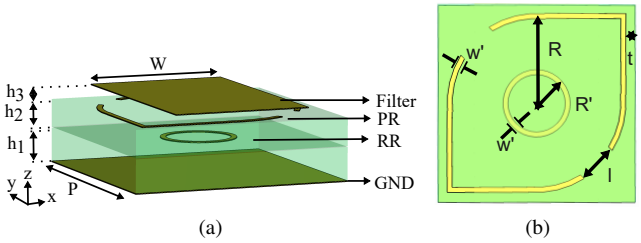


Fig. 2. (a) Unit cell. (b) Polarization rotator(PR) and ring resonator (RR) from top view. GND: ground. Period (P): 10 mm, filter width (W): 6.5 mm, edge clearance: t: 0.5 mm, substrate heights ($h_{1,2}$): 1.5 mm, 1.25 mm respectively, air gap h_3: 0.5 mm, split gap size (l): varying, PR radius (R): 4.5 mm, RR radius (R'): 1.7 mm. Copper trace width (w'): 250 μm. FR4 substrates (green), copper (yellow)

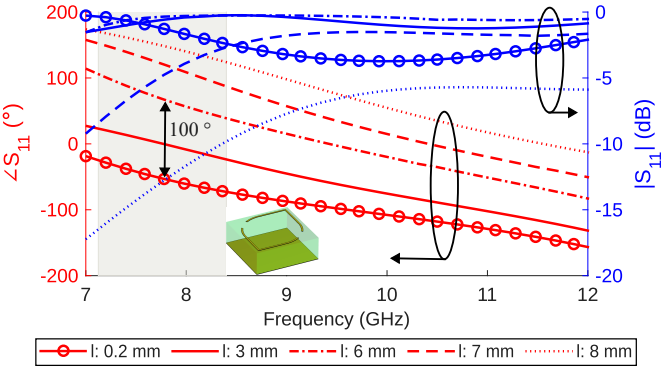


Fig. 3. Phase and amplitude of the polarization rotator for the cross polarization state at different values of l. The desired band is highlighted with gray rectangle. Substrate height: 3.2 mm

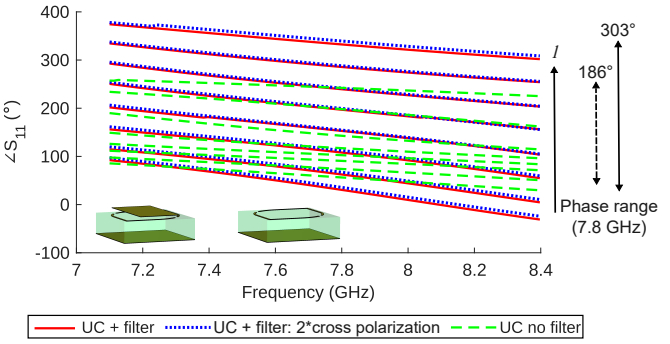


Fig. 4. Phase comparison of the 3-bit states for design including a filter (solid and dotted lines), and the design without filter (dashed lines). Both excited in TM mode. Small and large phase ranges are for unit cells (UC) without and with the filter respectively. 2* indicates the phase values multiplied by two. Each state is defined by a split gap size l shown in table I and the increasing order is shown by an arrow. Substrate height: 3.2 mm

7.8 GHz. We maintained an edge clearance of $t = 0.5$ mm to prevent coupling between adjacent cells. Note that to increase the benefit derived from the inductance, we extended the split ring toward the edges of the unit cell, resulting in a more diamond-like shape.

To separate the effect of the polarization rotator, we begin our unit cell analysis by excluding both the filter and the ring resonator from the design. All simulations in this section are

TABLE I
3-BIT CONFIGURATIONS OF FILTER INTEGRATED UNIT CELLS AT 7.8 GHZ

Bit state	0	1	2	3	4	5	6	7
ϕ	0	45	90	135	180	225	270	315
l (mm) without RR	1	2	3.4	4.3	5	5.6	6.4	8.2
l (mm) with RR	1	2.7	4	4.8	5.35	5.8	6.5	8.2

performed using a frequency domain solver with Floquet mode excitation under periodic boundary conditions. By varying the size of the split (l in Fig. 2(b)), both the line inductance and the capacitance formed across the split are reduced. This reduction collectively shifts the resonance frequency toward higher values, thereby adjusting the cross polarization phase as shown in Fig. 3. The results demonstrate a linear phase response across a wide frequency range.

The drawback of adjusting the l parameter is a significant loss of polarization rotation efficiency within the desired band. As depicted in Fig. 3, $|S_{11}|$ remains above -2 dB in the desired band, if l is smaller than 6 mm. This limit, yields only 100° of phase shift which is not enough for 3-bit resolution. However, integrating the filter improves substantially the $|S_{11}|$ which allows the expansion of the l range, hence the phase range. Figure 4 demonstrates that 303° of phase shift is achieved with each line representing one of the eight states of the 3-bit resolution. Table I presents these bit states, their ideal phase values (ϕ), and the corresponding l dimensions that achieve the closest phase approximation at 7.8 GHz. We currently focus on the design without the ring resonator. As depicted in Fig. 5, it exhibits for each bit state an $|S_{11}|$ above -0.9 dB in the desired band.

We now compare in Fig. 4 the phase shift performance using the same l dimensions in the Table I for the versions with and without the filter. The objective is to determine if the filter doubles the phase range. The version without the filter reaches 186° of phase shift. However, for the design with filter the maximum shift is 303° and not 372°. This indicates that the filter interaction with the polarization rotator cannot be neglected.

To confirm the phase doubling, we therefore focus only on the unit cell with the filter, by comparing its cross-polarization phase values, with the initial co-polarization phase. The result coincides perfectly with the total measured phase by taking twice the cross-polarization phase and adding 10° of offset. The offset is related to the gap between the filter and the polarization rotator. This demonstrates that the unit cell achieves exactly twice the phase shift provided by the polarization rotator while maintaining a high $|S_{11}|$ above -1 dB for the incident polarization and $|S_{11}|$ below -10 dB for the cross polarization.

Despite optimization efforts, the phase interval between bit states 0 and 1 exhibits significant deviation from the ideal 45° target, resulting in an error exceeding ±15°. To enhance

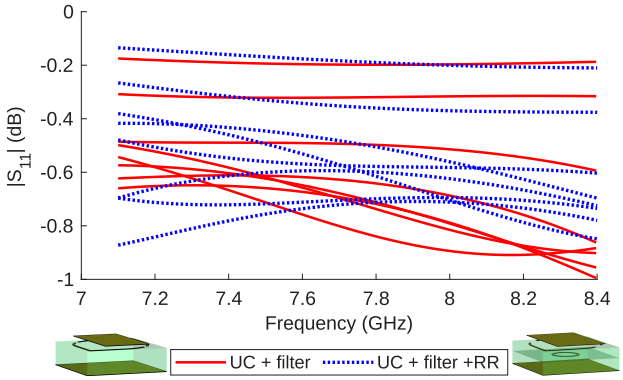


Fig. 5. Amplitude comparison of the 3-bit states for two different unit cell designs, both excited in TM mode: Design including a filter (solid lines), and the design including a filter, and a ring resonator (dotted lines). Substrate height: 2.75 mm and 3.2 mm for designs with and without RR respectively.

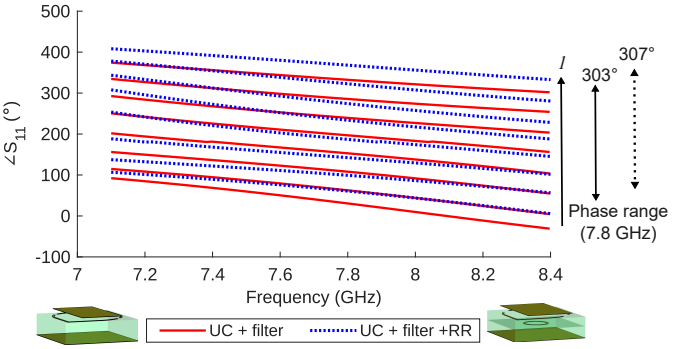


Fig. 6. Phase comparison of the design with and without the ring resonator for 3 bit states. Each state is defined by a split gap size l shown in table I and the increasing order is shown by an arrow. Substrate height: 2.75 mm and 3.2 mm for designs with and without RR respectively.

the phase linearity and minimize this error, we integrate a ring resonator at a fixed radius of 1.7 mm between the polarization rotator and the ground plane. The resonator creates an additional resonance outside of the desired band allowing to adjust the slope of the phase curves. This modification reduces the deviation mostly in the range of ±15° up to 20° between all bit states throughout the entire band and increases the phase range up to 307° at 7.8 GHz as shown in Figure 6. The final design is described in Fig. 2(a) with overall substrate height reduced down to 2.75 mm and l dimensions depicted in Table I. To further minimize the error, one could parametrize the radius R'. However, this would complicate the structure and is therefore beyond the scope of this paper. Figure 5 shows that all bit states have $|S_{11}|$ above -0.9 dB. Therefore, we proceed with a unit cell shown in Fig 2(a) with bit states defined in table I to construct the RIS panel.

III. RIS PANEL DESIGN

In this section, to validate the concept, the RIS panel is designed for one-dimensional (1D) beam scanning. As shown in Fig. 1(a), the RIS is constructed using repeated supercells which are a block of unit cells exhibiting a discretized linear phase profile for a specific deflection angle following the

TABLE II
SUPERCELL PHASE PROFILES AND CORRESPONDING BIT STATES FOR MULTIPLE DEFLECTION ANGLES AT 7.8 GHZ

10° $\Phi(°)$	0 16 33 49 65 81 98 115 131 147 164 180 196 213 229 245 262 278 295 311 327 344
10° *bits*	0 0 0 1 1 2 2 2 3 3 4 4 4 5 5 5 6 6 7 7 7 0
20° $\Phi(°)$	0 33 65 98 131 164 196 229 262 295 327
20° *bits*	0 0 1 2 3 4 4 5 6 7 7
30° $\Phi(°)$	0 45 90 135 180 225 270 315
30° *bits*	0 1 2 3 4 5 6 7
40° $\Phi(°)$	0 60 120 180 240 300
40° *bits*	0 1 3 4 6 7
50° $\Phi(°)$	0 72 144 216 288
50° *bits*	0 2 4 5 7

generalized Snell's law [4]. The required phase profile is mapped onto the available bit states in the Table I. Table II summarizes on the right column the discretized phase profile (Φ) with rounded values and corresponding bit states for the 10°, 20°, 30°, 40° and 50° deflection angles which are on the left column. Due to the decrease in discretization resolution for deflection angles above 30°, bit selection is optimized to minimize the grating lobes. Each RIS panel is formed by repeating supercells in this table and has 300×300 mm dimensions as shown in Fig. 1(a).

Simulations are realized with an FDTD solver of EMPIRE software under TM mode excitation. Across the entire desired band, RIS panel consistently provides a main lobe at the target angle. However, for visual clarity, a single deflection angle (30°) is chosen to demonstrate the bandwidth coverage and a single frequency (7.8 GHz) is selected to illustrate the beam scanning performance. Changing the orientation of the filter would provide the same results for the TE mode.

Figure 7 compares the deflection performance across the $7.1 - 8.4$ GHz range for a fixed deflection angle of 30°. We observe that the main lobe gain remains above 15.5 dB and is closely aligned with the desired angle, showing only small angular shifts due to wavelength variation across the band. Furthermore, the achieved side lobe levels (SLL) is below -12 dB. These results demonstrate that the RIS design provides adequate performance and stability throughout the entire operational bandwidth. Note that for larger deflection angles, grating lobes remain above -10 dB, up to -7.5 dB towards the extremities of the band. This is because of the discretization resolution of the phase profile and can be solved by reducing the periodicity of the unit cell.

Figure 8 compares the beam scanning performance of the RIS against a reference copper metallic plate of the same surface area. The main lobes closely follow the theoretical scan loss curve, exhibiting a maximum difference of -1.1 dB. This confirms the high efficiency of the structure and its ability to support beam deflection up to 50°.

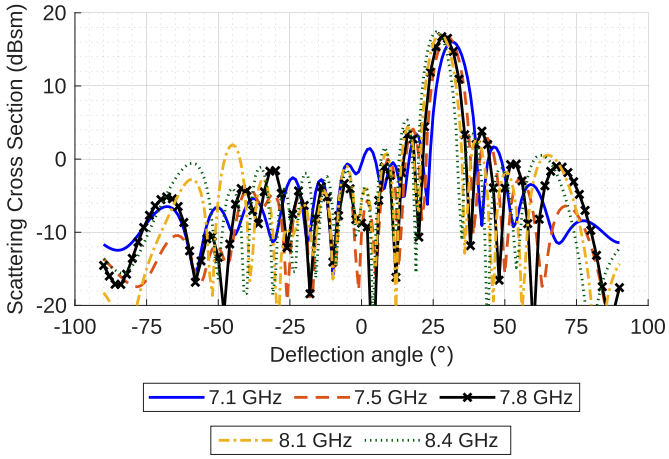


Fig. 7. Radiation pattern at different frequencies of RIS designed for 30° deflection angle.

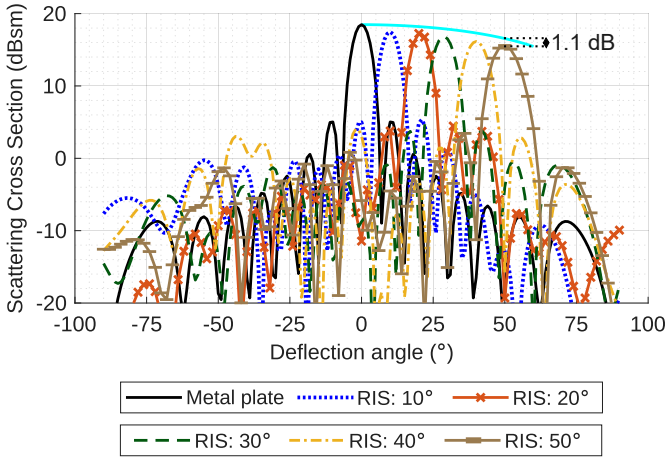


Fig. 8. Beam scanning at 7.8 GHz for different deflection angles. Scan loss (solid cyan line) calculated with respect a copper plate having the same surface as RIS.

IV. CONCLUSION AND PERSPECTIVES

In this work, we presented a novel 3-bit RIS panel design that integrates polarization rotation and a filter to achieve enhanced linear phase range and efficiency via internal reflections. The unit cell exhibits high efficiency with $|S_{11}|$ above -0.9 dB and a wide operational range across the entire $7.1 - 8.4$ GHz band, while maintaining a significant phase shift capability up to 307° at the central frequency. These combined properties successfully demonstrate a RIS panel achieving an excellent agreement with the theoretical scan loss up to 50° of beam deflection with a maximum 1.1 dB of difference. Despite lossy FR4 substrate and copper materials, it achieves a stable and high-performance operation across the entire band. Therefore, our novel concept, offers a promising and cost-effective solution for high-efficiency, wideband beam deflection in the FR3 band, positioning it as a strong candidate for future 6G applications. Upcoming research will target the implementation of this same concept based on unit cells with active components to achieve real-time reconfigurability.

ACKNOWLEDGMENT

This publication is based upon work supported by the Horizon Europe Research and Innovation Program and UKRI under the GENIUS Project, Marie Skłodowska-Curie Grant under Agreement 101072560.

REFERENCES

[1] W. Long, R. Chen, M. Moretti, W. Zhang, and J. Li, "A Promising Technology for 6G Wireless Networks: Intelligent Reflecting Surface," *Journal of Communications and Information Networks*, vol. 6, no. 1, pp. 1–16, 2021.

[2] T. Huang, W. Yang, J. Wu, J. Ma, X. Zhang, and D. Zhang, "A Survey on Green 6G Network: Architecture and Technologies," *IEEE Access*, vol. 7, pp. 175 758–175 768, 2019.

[3] Z. Cui, P. Zhang, and S. Pollin, "6G Wireless Communications in 7–24 GHz Band: Opportunities, Techniques, and Challenges," in *2025 IEEE International Symposium on Dynamic Spectrum Access Networks (DySPAN)*, 2025, pp. 1–8.

[4] L. Zheng and Y. Zhao, "Generalized Snell's Law and Its Verification by Metasurface," in *Innovative Mobile and Internet Services in Ubiquitous Computing*, L. Barolli, A. Poniszewska-Maranda, and H. Park, Eds. Cham: Springer International Publishing, 2021, pp. 364–372.

[5] S. Rana, Y. S. Sreenija, S. Kumar, and A. R. Harish, "1.5-bit Passive RIS for Single Beam Anomalous Reflection," in *2024 IEEE Microwaves, Antennas, and Propagation Conference (MAPCON)*, 2024, pp. 1–4.

[6] S. Finich, N. A. Touhami, and A. Farkhsi, "Design and Analysis of Different Shapes for Unit-Cell Reflectarray Antenna," *Procedia Engineering*, vol. 181, pp. 526–530, 2017, 10th International Conference Interdisciplinarity in Engineering, INTER-ENG 2016, 6-7 October 2016, Tirgu Mures, Romania. [Online]. Available: https://www.sciencedirect.com/science/article/pii/S1877705817310135

[7] S. Siddha, A. Rahman, and R. R. Mahmud, "Design of X-Band Reflect Array Antenna using Circular Ring Patches," in *2021 3rd International Conference on Electrical & Electronic Engineering (ICEEE)*, 2021, pp. 49–52.

[8] T. Shabbir, M. T. Islam, N. Misran, S. S. Al-Bawri, and S. Singh, "Broadband single-layer reflectarray antenna loaded with meander-delay-lines for X-band applications," *Alexandria Engineering Journal*, vol. 60, no. 1, pp. 1105–1112, 2021. [Online]. Available: https://www.sciencedirect.com/science/article/pii/S1110016820305421

[9] M. Saikia, S. Ghosh, S. Bhattacharyya, and K. V. Srivastava, "Broadband polarization rotator using multilayered metasurfaces," in *2015 IEEE Applied Electromagnetics Conference (AEMC)*, 2015, pp. 1–2.

[10] A. A. Omar, "Reflective and Transmissive Linear Polarization Rotators: A Review," *IEEE Open Journal of Antennas and Propagation*, vol. 6, no. 3, pp. 633–644, 2025.

[11] L. Gao and L. Guo, "A Low-Profile Reflect-Transmit-Array Antenna Using Polarization Rotating Unit Cells," in *2023 International Conference on Microwave and Millimeter Wave Technology (ICMMT)*, 2023, pp. 1–3.

[12] A. Gayan, J. Das, and N. S. Bhattacharyya, "Dual Band Shared Aperture Polarization Converting Reflectarray for Independent Beamforming in C and X Bands," in *2025 IEEE Wireless Antenna and Microwave Symposium (WAMS)*, 2025, pp. 1–5.